Earth and Planetary Science Letters 444 (2016) 192–204

Contents lists available at ScienceDirect

Earth and Planetary Science Letters

www.elsevier.com/locate/epsl

Quantification of tsunami-induced flows on a Mediterranean carbonate ramp reveals catastrophic evolution

Arnoud Slootman [a,*], Matthieu J.B. Cartigny [b], Andrea Moscariello [a], Massimo Chiaradia [a], Poppe L. de Boer [c]

[a] Department of Earth Sciences, University of Geneva, Rue des Maraîchers 13, Geneva 1205, Switzerland
[b] National Oceanography Centre, University of Southampton Waterfront Campus, Southampton SO14 3ZH, UK
[c] Faculty of Geosciences, Utrecht University, PO Box 80.115, 3508 TC Utrecht, The Netherlands

ARTICLE INFO

Article history:
Received 26 August 2015
Received in revised form 31 March 2016
Accepted 31 March 2016
Editor: M. Frank

Keywords:
carbonate ramp
Mediterranean
tsunami
storm
supercritical flow
catastrophic evolution

ABSTRACT

Cool-water carbonates are the dominant limestones in the Mediterranean Basin since the Early Pliocene. Their deposition typically resulted in ramp morphologies due to high rates of resedimentation. Several such fossil carbonate ramps are characterised by a bimodal facies stacking pattern, where background deposition of subaqueous dune and/or tempestite deposits is repeatedly interrupted by anomalously thick sedimentary units, dominated by backset-stratification formed by supercritical flows. A multitude of exceptional triggers (e.g. storms, floods, tsunamis) have been invoked to explain the origin of these supercritical flows, which, in the absence of a quantitative analysis, remains speculative as yet. Here, for the first time, the catastrophic evolution of one such Mediterranean carbonate ramp, on Favignana Island (Italy), is quantified by combining $^{87}Sr/^{86}Sr$ dating, outcrop-based palaeoflow reconstructions and hydraulic calculations. We demonstrate that rare tsunami-induced flows, occurring on average once every 14 to 35 kyr, lasting a few hours only, deposited the anomalously thick backset-bedded units that form half of the sedimentary record. In between such events, cumulative two years of storm-induced flows deposited the remaining half of the succession by the stacking of subaqueous dunes. The two to four orders of magnitude difference in average recurrence period between the two flow types, and their associated sedimentation rates, emphasises the genetic differences between the two styles of deposition. In terms of sediment transport, the studied carbonate ramp was inactive for at least 99% of the time with gradual progradation during decennial to centennial storm activity. Carbonate ramp evolution attained a catastrophic signature by the contribution of rare tsunamis, producing short-lived, high-energy sediment gravity flows.

1. Introduction

Cool-water carbonates in shallow, temperate seas are characterised by the Heterozoan Association of James (1997), consisting largely of the remains of red algae, bivalves, bryozoans, echinoids and larger foraminifera, in the general absence of non-skeletal grains. They lack the major bioconstructions and early cementation typical of their tropical counterparts (Ahr, 1973; Carannante and Simone, 1988). The skeletal debris-covered sea floors thus formed are prone to remobilisation and hence have a reduced capacity to accumulate above storm wave base (Pomar and Tropeano, 2001), which may lead to the development of distally steepened ramp profiles (Pomar et al., 2002; Pedley and Carannante, 2006) (Fig. 1B). Skeletal sand and gravel produced on the ramp top in the unprotected carbonate factory are transported downramp by incidental currents, sweeping sediment below wave base. This results in the occasional deposition of bioclastic material on the ramp slope, leading to carbonate ramp progradation through the formation of large-scale clinoform units up to tens of metres high.

The sedimentary record of the Mediterranean Basin contains numerous examples of clinoform successions created in this way (e.g. Hansen, 1999; Pomar and Tropeano, 2001; Pomar et al., 2002; Puga-Bernabéu et al., 2010; Massari and D'Alessandro, 2012), forming up to six-storey vertical stacks where carbonate ramps originated in tectonically active areas, such as the Lower Pleistocene foreland and satellite basins of Sicily (e.g. Catalano et al., 1998; Massari and D'Alessandro, 2012). These clinoform successions, which prograded up to 1–2 km with a maximum height of several tens of metres, were suggested to correlate with the 41-kyr orbital obliquity-forced oscillation of global sea level related to the

* Corresponding author.
E-mail address: Arnoud.Slootman@unige.ch (A. Slootman).

http://dx.doi.org/10.1016/j.epsl.2016.03.052
0012-821X/

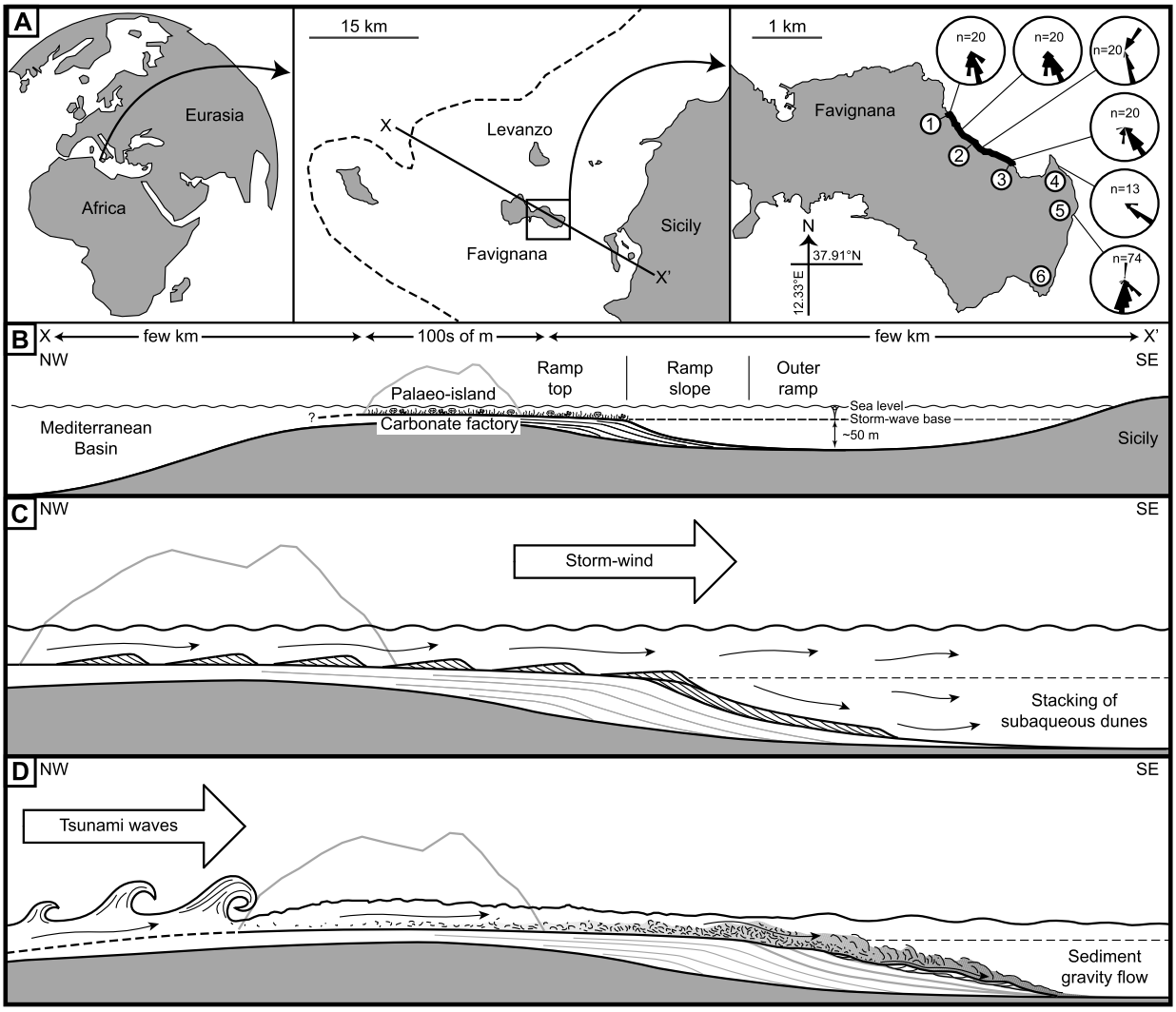

Fig. 1. Geography and conceptual cross-section of Favignana Island. (A) The study area (framed) is located offshore western Sicily in the central Mediterranean Basin. Dashed line indicates the present-day shelf (200 m isobath). The large sea cliff (Fig. 2) is highlighted by the thick line on the NE coast of the island. Rose diagrams each represent *n* measurements of the palaeoflow direction of subaqueous dune deposits in two dune cross-bedded clinoform units. Palaeoflow direction suggests that the clinoform succession of the Favignana carbonate ramp prograded approximately towards SE, away from and sourced by a palaeocarbonate factory between the islands of Favignana and Levanzo. Encircled numbers show strontium isotope stratigraphy sample locations; see also Table S1 in Supplementary Material. (B) Schematic cross-section displaying sub-environments on the carbonate ramp and the location of the palaeo-island (projected). (C) Depositional model for dune cross-bedded clinoform units, formed by the migration of subaqueous dunes during storm-driven, wind-induced currents. (D) Depositional model for backset-bedded clinoform units, deposited by tsunami-induced sediment gravity flows.

waxing and waning of Early Pleistocene northern hemisphere ice sheets (Catalano et al., 1998).

Individual clinoform units, which thus encompass the key architectural elements of carbonate ramp clinoform successions, typically consist of bioturbated tempestite and/or cross-bedded deposits (e.g. Hansen, 1999; Puga-Bernabéu et al., 2010; Massari and D'Alessandro, 2012), the latter formed by the downramp migration of subaqueous dunes (*sensu* Ashley, 1990). In addition, several Neogene–Quaternary carbonate ramp successions in the Mediterranean Basin comprise various proportions of clinoform units of anomalously thick, erosion-based sets displaying a poorly pronounced, upslope-dipping stratification in concave-up scours (e.g. Hansen, 1999; Pomar et al., 2002; Andreetta et al., 2008; Massari and D'Alessandro, 2012). Such sedimentary structures are commonly interpreted as backset-beds resulting from hydraulic jumps in submerged particulate gravity flows at the transition from erosive, Froude-supercritical flow to depositional, subcritical flow (Massari, 1996; Cartigny et al., 2014). A number of extreme events were proposed to have triggered such flows, including exceptional storms, strong floods and tsunamis.

This paper aims to provide a quantitative analysis of the origin of (1) backset-bedded deposits and (2) subaqueous dune cross-bedded/tempestite deposits on Mediterranean carbonate ramps, to clarify the relationship between the anomalous backset-bedded units and their background sediments. Using strontium isotope stratigraphy, outcrop-based palaeoflow reconstructions and hydraulic relations, we estimate the average recurrence periods and flow durations of the events linked to both types of deposits in the ramp succession of Favignana Island. On the basis of original data presented here, deposition of the studied succession is constrained within several hundred kyr. Furthermore, over an average period of 14–35 kyr half of the deposits formed during a cumulative two years of storm-induced currents, while the remaining half was deposited in less than six hours by a single, high-energy flow.

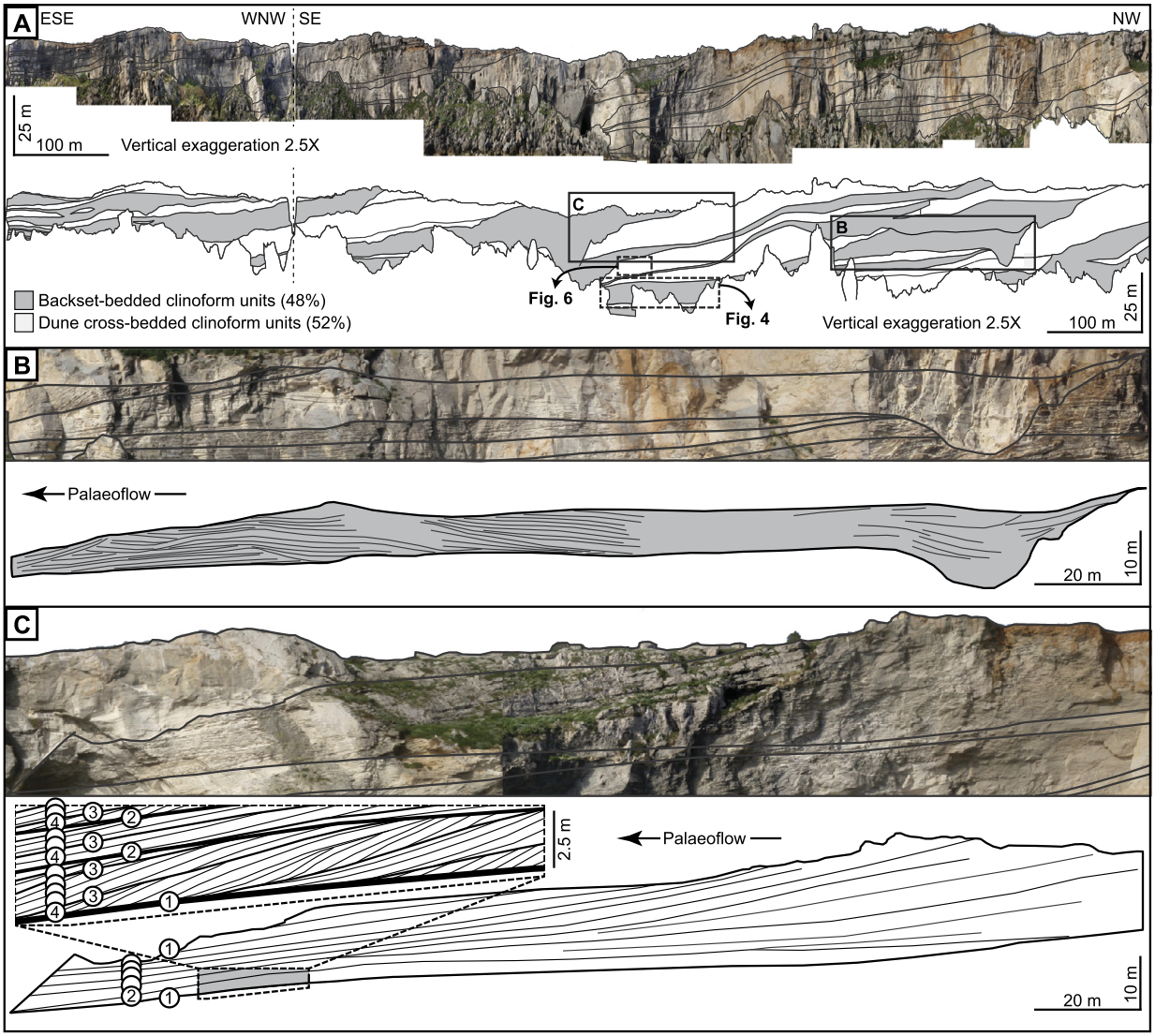

Fig. 2. Sea cliff section displaying clinoform architecture and close-ups. For location see Fig. 1. (A) Photo panel and line drawing showing first order boundaries between clinoform units. Note 2.5× vertical exaggeration. (B) Photo panel and line drawing of the proximal section of the examined backset-bedded clinoform unit. Note erosional character of the base. (C) Photo panel and line drawing of dune cross-bedded clinoform unit. Encircled numbers indicate hierarchy of bounding surfaces: (1) clinoform unit boundary; (2) set boundary; (3) compound cross-bed boundary; (4) cross-bed boundary.

2. Geological setting

Favignana (18 km^2) is the principal island of the Aegadian Archipelago, offshore western Sicily (Fig. 1A). The region belongs to the Alpine collision belt along the African–European plate boundary, characterised by the superposition of thrust sheets since Miocene times, on the front of which the Favignana wedge-top basin developed (Catalano et al., 2002). The (palaeo-)island's main topographic feature is a ridge of tectonically emplaced Triassic to Miocene sedimentary rocks (Tavarnelli et al., 2003). At either side, Pleistocene calcarenites and calcirudites, overlying Pliocene marlstones, are largely unaffected by tectonic deformation. The age of the uppermost interval of the exposed marlstones is bracketed between the Last Occurrence (LO) of the foraminifera marker species *G. sphaeroidinellopsis seminulina* (3.19 Ma) and the LO of *G. bononiensis* (2.41 Ma). These marlstones, therefore, belong to the Monte Narbone Formation of southern Sicily (Catalano et al., 1998). The Pleistocene calcarenites and calcirudites, which are the topic of the present study, have hitherto not been dated. They comprise coarse-grained Heterozoan skeletal pack- and grainstones (1–2% non-carbonate particles), with locally abundant gravel-size bioclasts. Quarries scattered across the island and a large sea cliff of seismic-scale dimensions (1.2 km by 50 m) offer textbook exposures (Fig. 2). The studied deposits have been previously interpreted as the sedimentary record of an ancient shoreface cross-cut by channels (Ślączka et al., 2011).

The calcarenites and calcirudites of Favignana pass from tabular, low-angle shoreface packages onlapping the ridge, into a succession of SE prograding ramp slope clinoform units up to 50 m high, 500 m long and tens of m thick, dipping about 5–20 degrees (Fig. 2). Clinoform units progressively thicken from their most proximal location in the vicinity of the ridge towards the large sea cliff along the NE coast of the island in which clinoform units reach their maximum thickness and inclination. Ca. 50% of the clinoform succession is composed of bioturbated (*Thalassinoides*), high-angle cross-stratified calcarenites and calcirudites formed by the S/SE migration of subaqueous dunes (Fig. 1). Such dunes migrated down the ramp slope under the influence of currents undergoing a slight deflection to the right (cf. Massari and D'Alessandro, 2012), most likely imposed by the Coriolis force (e.g. Puga-Bernabéu et al., 2010). The prograding, high-angle cross-bedded bodies, formed by downslope-migrating subaqueous dunes, are here referred to as

'dune cross-bedded clinoform units'. The succession of dune cross-bedded clinoform units is repeatedly interrupted by up to 10 m thick, erosion-based sandy to gravelly clinoform units composed of amalgamated sets of backset-bedded deposits (grey in Fig. 2), ascribed to the cyclic formation by numerous hydraulic jumps (cf. Cartigny et al., 2014). Such prograding bodies are here referred to as 'backset-bedded clinoform units', which are best developed in slope and outer ramp settings and pinch out basinwards. They contain rare escape burrows (*Ophiomorpha*) and accumulations of large *ex situ* bioclasts up to 15 cm in diameter. These backset-bedded clinoform units comprise the remaining half of the sedimentary record.

A clinoform couplet is defined as the combination of one dune cross-bedded clinoform unit and one backset-bedded clinoform unit. The clinoform succession of Favignana Island contains ca. 35 of such clinoform couplets, the thickest and steepest of which crop out in the large sea cliff shown in Fig. 2. The distal termination of the succession in the SE reflects the final position reached by progradation. The clinoform succession is believed to have originally extended towards the inferred carbonate factory on the submarine high between the islands of Favignana and Levanzo (Fig. 1).

3. Methods

To unravel the nature and timing of the events that built the Favignana carbonate ramp succession, three time scales need to be constrained: (1) time contained within one clinoform couplet, (2) duration of flow events associated with the deposition of individual backset-bedded clinoform units, and (3) cumulative time required to construct the deposits of a single dune cross-bedded clinoform unit. The time scale for deposition of one clinoform couplet was obtained from strontium isotope stratigraphy. Flow duration associated with individual clinoform units was estimated by dividing sediment volume by their respective fluxes, which follow from palaeohydraulic reconstructions.

3.1. Strontium isotope stratigraphy

Strontium isotope stratigraphy is based on direct comparison of measured $^{87}Sr/^{86}Sr$ in a sample to the known $^{87}Sr/^{86}Sr$ variation in sea water calibrated through time (Smalley et al., 1994; McArthur et al., 2012). This method thus requires the measurement of strontium isotope ratio in minerals that precipitated from sea water, such as biogenic calcite, which have not been diagenetically altered. Quaternary $^{87}Sr/^{86}Sr$ variation is characterised by a rapid monotonous increase, making this period very suitable for strontium isotope dating (McArthur et al., 2012). Samples of red algal composition are recognised as highly reliable in recording the original sea water strontium isotope ratio, but nonetheless need to undergo a screening procedure to determine the state of sample preservation (Smalley et al., 1994).

Six stratigraphically distributed sample locations were selected, comprising a succession of 20 clinoform couplets in the large sea cliff and the eastern part of the island (Fig. 1A). From each location ten fossil rhodoliths (red algal spheres) with a minimum diameter of 5 cm were collected. After superficial cleaning with a brush and ultrasonic bath, each rhodolith was carefully fragmented into 5–10 mg pieces. Subsequently, about 50 mg of each sample was hand-picked using a binocular microscope. Criteria for selection were the absence of sand grains, the absence of visible non-primary minerals, and the absence of visible, recent organic contamination. For each of the 60 rhodoliths, one fragment was mounted on a conductive aluminium support with double-sided conductive carbon tape. An ultra-thin, ca. 10 nm gold coating was then deposited on the samples by low vacuum sputter coating prior to imaging with a Jeol JSM 7001F Scanning Electron Microscope (SEM). A semi-qualitative scheme was developed for the assessment of the petrographic state of sample preservation. Thirteen out of the 60 samples passed the SEM screening test and were subsequently prepared for $^{87}Sr/^{86}Sr$ measurement (see Supplementary Material for details). $^{87}Sr/^{86}Sr$ was measured with a Thermo Neptune PLUS Multi-Collector ICP-MS in static mode. Long-term (over one year) external reproducibility of the SRM987 standard on the mass spectrometer is 7 ppm (one standard deviation).

Each of the thirteen samples was measured multiple times; hence the results consist of thirteen sample mean $^{87}Sr/^{86}Sr$ values and accompanying sample standard deviations. The table of McArthur et al. (2012) gives the mean, lower limit and upper limit $^{87}Sr/^{86}Sr$ value corresponding to a 95% confidence interval with time steps of 50 kyr, which were decreased to increments of 10 kyr by linear interpolation. Following the guidelines of McArthur et al. (2012) and assuming normal distribution of errors, each sample was assigned an estimated mean age and a standard deviation. For each sample the cumulative probability for every possible combination of age (Ma) and duration (i.e. time span (kyr) in which all samples were deposited) were calculated, in order to answer the question: What is the probability $P_{i,T,t}$ that sample i, with mean age μ_i and standard deviation σ_i, was deposited within a period of T kyr beginning at time t Ma? Subsequently, the cumulative probability of all samples for every possible combination of T and t was obtained by calculation of the product of $P_{i,T,t}$ for i that goes from 1 to 13 (see Supplementary Material for details). The results are close to but not normally distributed.

3.2. Duration of flow events

A scale order for the duration of flow events was estimated by dividing cross-sectional sediment volume by sediment discharge per unit width (i.e. specific sediment discharge), derived from palaeohydraulic reconstructions. The flow-parallel cross-sectional area of the different clinoform units was measured from the cliff section in Fig. 2. Specific sediment discharge is the product of average flow velocity, flow thickness and sediment concentration. For dune cross-bedded clinoform units, the link between sedimentary structures and flow properties was quantified using the field-based bedform stability diagram of Van den Berg and Van Gelder (1993). Associated sediment fluxes were calculated with classical sediment transport predictors for bed-load-dominated transport (Meyer-Peter and Mueller, 1948). For backset-bedded clinoform units, on the other hand, the experimental relation between antidune length, flow velocity and flow thickness was used (Kennedy, 1963; Hand, 1974; Cartigny et al., 2014). These experimental relations were previously validated in modern environments by e.g. Alexander and Fielding (1997), who showed that the wavelength of gravel antidunes in a bankfull tropical river correspond to flow depth and velocity. Backset-bedding formed predominantly under suspension load transport, hence on the basis of previous experimental work (Cartigny et al., 2013), which links sediment concentration-dependent turbulence damping to the formation of 'spaced stratification' (*sensu* Hiscott, 1994), sediment concentrations were inferred from this type of stratification observed in outcrop. The experimentally derived relations can be applied on a field-scale as demonstrated by Cartigny et al. (2013) and are therefore justifiably used here to estimate the duration of flow events.

The transport of bed and suspended load was derived using models for siliciclastic particles. Physical experiments, however, have shown that biogenic carbonate sands have lower mobility thresholds and settling velocities than siliciclastic grains, due to differences in grain shape, density and intragranular porosity (Prager et al., 1996; Smith and Cheung, 2004, and refs. therein). Initiation of motion of carbonate particles was found to occur for

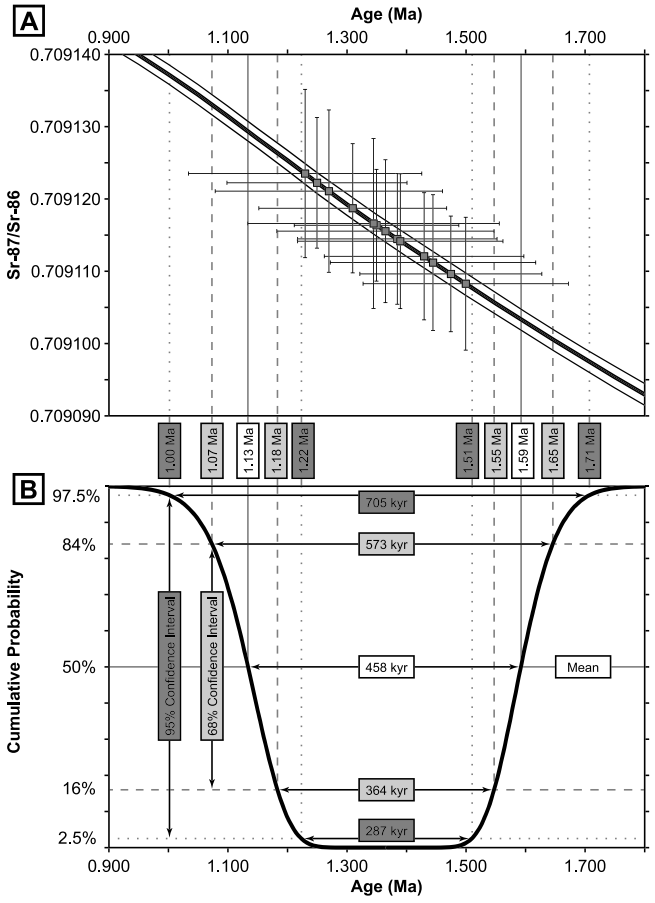

Fig. 3. Results of strontium isotope stratigraphy of an interval comprising 20 clinoform couplets within the Pleistocene carbonate ramp succession of Favignana Island. (A) $^{87}Sr/^{86}Sr$ values of thirteen fossil rhodolith samples (Table S1) plotted on the LOWESS best-fit curve (Skeleton Version 5) for strontium isotope ratios as a function of time (thick line: mean age; thin lines: limits of the 95% confidence interval) calibrated by McArthur et al. (2012). Error bars show the 95% confidence interval for each sample corresponding to two standard deviations. (B) Cumulative probability of lower and upper age limits of the sampled stratigraphic interval. A larger confidence interval corresponds to wider ranges of the lower and upper age limit, thereby increasing the possible range of the time contained within the sampled clinoform succession (i.e. duration). For example, on a 95% confidence level, deposition of the sampled stratigraphic interval lasted between 287 and 705 kyr, commencing between 1.71 and 1.51 Ma and ending between 1.22 and 1.00 Ma.

mobility parameters (*sensu* Van Rijn, 1984) up to ca. 25% lower than those typical for siliciclastic particles. The mobility difference between carbonate and siliciclastic sands is, however, less than the precision in the lower ranges of the available siliciclastic models. Hence, use of the above methods is justified, as the outcome of the present study is not significantly affected by the difference in hydrodynamic behaviour between siliciclastic and carbonate particles.

4. Results

4.1. Strontium isotope stratigraphy

The thirteen fossil rhodolith samples from a succession of 20 clinoform couplets range in age from 1.500 to 1.230 Ma (Fig. 3A, Table S1 in Supplementary Material). Due to an average uncertainty of ca. ±170 kyr (95% confidence level) on the age of individual samples, mean ages do not plot in the chronological order inferred from their stratigraphic position. However, the objective of $^{87}Sr/^{86}Sr$ dating was not to constrain individual sample ages, but to investigate the time contained within the clinoform succession. The measured time span for deposition of the studied succession is controlled by the confidence level; larger confidence intervals result in upper and lower limits farther removed from the median duration of 458 kyr. On a 95% confidence level, the duration of deposition of all samples is between 287 and 705 kyr, a period that began between 1.71 and 1.51 Ma and ended between 1.22 and 1.00 Ma (Fig. 3B), confirming the assumed Lower Pleistocene age (Ślączka et al., 2011). This time span is larger than that of the typical clinoform successions of the Lower Pleistocene of Sicily (ca. 41 kyr, Catalano et al., 1998; Massari and D'Alessandro, 2012), implying a deviating evolution of the Favignana system compared to the regional standard model. Since the sampled succession contains 20 clinoform couplets, deposition of each clinoform couplet covered an average time span of 14 to 35 kyr, which thus represents the average recurrence period of backset-generating events and the average time comprised within a dune cross-bedded clinoform unit.

4.2. Anomalous backset-bedded clinoform units

4.2.1. Sedimentary features

The backset-bedded clinoform units outcropping in the large sea cliff (Fig. 2) display very similar architecture and facies, despite their variation in thickness. They consist invariably of amalgamated sets of backset-bedding. The lower boundary of backset-bedded clinoform units is typically increasingly erosive towards the proximal ramp slope, where these units are up to 10 m thick (Fig. 2). Large variations in grain size occur throughout the units, ranging from sand to gravel. The near absence of bioturbation emphasises the event character and rapid deposition of backset-bedded clinoform units, with escape burrows (*Ophiomorpha*) being rarely present in the uppermost interval. Although individual backset-bedded sets formed by the scouring and filling associated with a single hydraulic jump (cf. Massari, 1996), the generation of a backset-bedded clinoform unit is related to the repetitive formation of numerous hydraulic jumps during a single sediment gravity flow event, in which part of the backset-dominated stratification passes from one set into the other generating an amalgamated stacking pattern of backset-bedded sets (cf. Cartigny et al., 2014). The backset-bedded clinoform units together comprise about half of the thickness of the studied succession (Fig. 2).

One backset-bedded clinoform unit with high exposure quality and easy accessibility was investigated in more detail. This unit dips slightly oblique to the outcrop and parallel to clinoform progradation and palaeotransport. It is up to 7 m thick in the studied section and can be traced over 400 m updip (Figs. 2 and 4; high-resolution photo available through Supplementary Material). The lower part consists of a set of coarse sand- to granule-grained backset-beds, which dip gently upstream and become progressively wavier upwards. The contact with the overlying backset-bedded set with gravel-sized bioclasts is erosive, culminating in a 3 m-deep, asymmetric scour filled with backset-bedding, in which each subsequent backset-bed truncates the preceding one progressively farther upstream, generating a composite erosion surface and an apparent onlap onto the upstream side of the scour (Fig. 5).

4.2.2. Palaeohydraulic reconstruction

The preserved wavy geometries are explained as the result of progressively steepening antidunes that formed on the stoss-side of a larger bedform (Figs. 5B–C), generated by a gravity flow rushing down the ramp slope. The combination of severe erosion and deposition of backset-stratification, points to hydraulic jumps and breaking waves (Figs. 5D–G), as expected in steepening antidune sequences (cf. Kennedy, 1963; Hand, 1974; Cartigny et al., 2014). Mean flow velocity U is related to antidune wavelength L (Hand, 1974) by

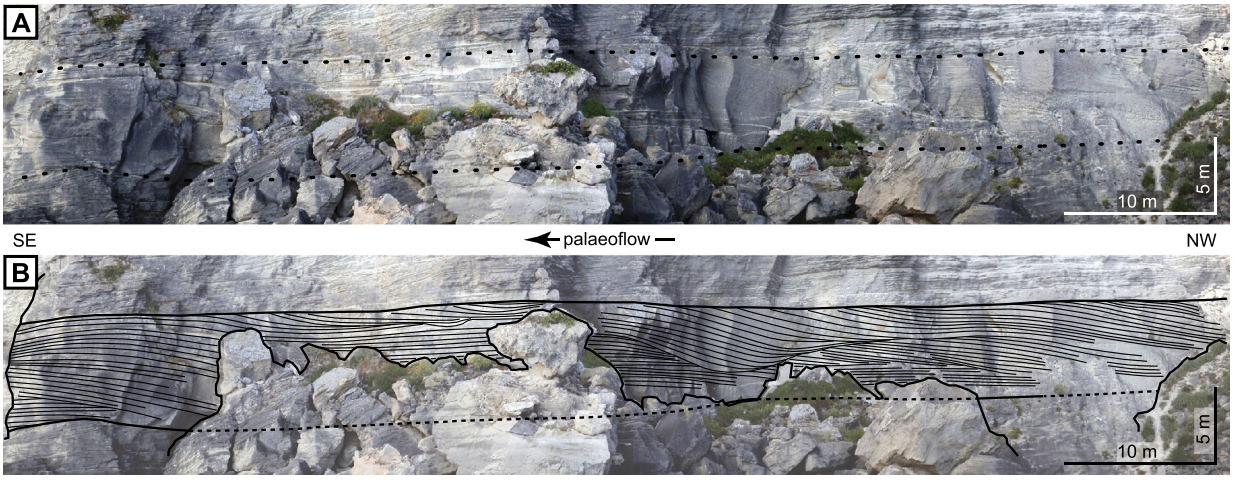

Fig. 4. Analysed section of the examined backset-bedded clinoform unit. Close-up of Fig. 2. (A) Photo panel. Dotted lines indicate upper and lower boundaries of the studied unit. (B) Line drawing of internal stratification. Part of the outcrop is not visible in the photo panel due to recent debris in front of the exposure. However, the exposure is for a large part accessible behind the scree. Such additional data were used in the palaeohydraulic reconstruction of Fig. 5.

Table 1
Flow parameters associated with the deposition of backset-bedded and dune cross-bedded clinoform units.

Deposition of studied backset-bedded clinoform unit

Description	Symbol	Unit	Flow 1	Flow 2	Flow 3
Sediment concentration flow	C_{flow}	%	4.5	10.0	15.0
Sediment concentration ambient/low-density layer	C_{amb}	%	0.0	4.5	4.5
Mean flow velocity over antidunes (Hand, 1974)	U	m/s	1.2	1.3	1.8
Average flow thickness	d	m	1.9	1.9	2.0
Flow duration for examined backset-bedded clinoform unit	t	h	6.2	2.6	1.2

Deposition of equivalent dune cross-bedded clinoform unit

Description	Symbol	Unit	Case 1	Case 2	Case 3
Mobility parameter (Van Rijn, 1984)	θ'	(–)	0.15	0.2	0.5
Flow velocity in 50 m water depth	U_{50}	m/s	1.4	1.6	2.6
Flow velocity in 100 m water depth	U_{100}	m/s	1.5	1.7	2.7
Cumulative flow duration for dune cross-bedded clinoform unit	$t_{cum.}$	days	838	463	91
Average flow duration single dune-activating event (in case of 50 events)	$t_{single,n=50}$	days	16.8	9.3	1.8
Average flow duration single dune-activating event (in case of 500 events)	$t_{single,n=500}$	days	1.7	0.9	0.2

$$U = \sqrt{\frac{gL}{2\pi}\frac{\rho_{flow} - \rho_{amb}}{\rho_{flow} + \rho_{amb}}} \quad (1)$$

where g is acceleration of gravity, and ρ_{flow} and ρ_{amb} are the densities of the flow and the ambient water. The density of the flow is a direct function of its sediment concentration, which is reflected in the stratification type of individual backset-beds (Cartigny et al., 2013). The preserved spaced stratification (*sensu* Hiscott, 1994) consists of cm-thick strata separated by erosion surfaces. This suggests a reduced turbulence at the base of the flow that prevented the deposition of mm-thick upper-stage plane-bedding, while maintaining enough turbulence to allow shear-stress pulses, generated higher in the flow, to cause intervals of bed erosion. This points to basal sediment concentrations between 5 and 15% by volume (Cartigny et al., 2013). Above a 9% threshold of sediment concentration (Bagnold, 1954) a dense basal layer develops. Such flow stratification should be accounted for in the calculations, by replacing the ambient fluid density by the density of a dilute, overriding layer. Following Bagnold (1954) such dilute layer has a sediment concentration of 9% at its base (interface with dense basal layer) and 0% at its top (ambient water). As an approximation a linear sediment concentration profile is assumed; hence average sediment concentration of a dilute layer is 4.5%. Using the measured antidune wavelength of 28 m (Fig. 5) and the relation of Hand (1974), the velocities of three flows of different sediment concentration (4.5%, 10%, 15%) were estimated between 1.2 and 1.8 m/s (Table 1).

Laboratory experiments have shown that specific bedforms are linked to distinct ranges of the densiometric Froude number Fr' (Hand, 1974; Cartigny et al., 2014);

$$Fr' = \frac{U}{\sqrt{g'd}} \quad (2)$$

where g' is submerged gravity ($g' = g[\rho_{flow} - \rho_{amb}]/\rho_{flow}$) and d is flow thickness. Antidunes associated with breaking waves form at densiometric Froude numbers of about $Fr' = 1.1$ (Cartigny et al., 2014), corresponding to a flow thickness of ca. 2 m (Table 1).

Sediment flux q_s (m^2/s) is defined as the amount of sediment passing a vertical line on the slope per unit time. It equals the product of flow velocity, flow thickness and sediment concentration C_{flow}. Flow duration can now be estimated by dividing the dip-parallel, cross-sectional area of the examined backset-bedded clinoform unit ($A \approx 2400$ m^2) by sediment flux;

$$t = \frac{A}{q_s} = \frac{A}{UdC_{flow}} \quad (3)$$

These calculations show that the sediment gravity flows associated with the generation of backset-bedded clinoform units lasted a few hours only (1–6 hrs, Table 1).

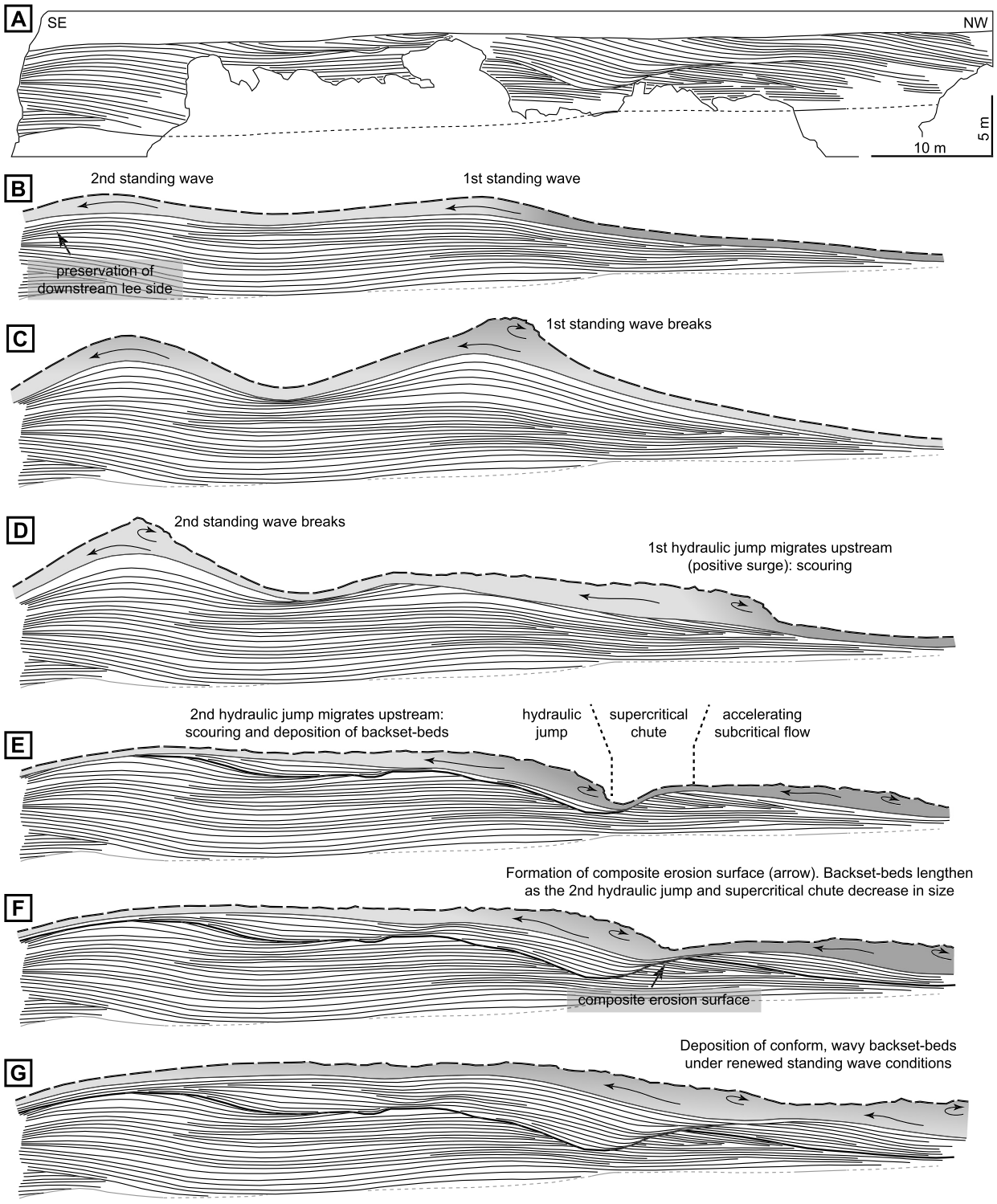

Fig. 5. Palaeohydraulic reconstruction of the studied section of the examined backset-bedded clinoform unit. (A) Line drawing of internal stratification. See also Fig. 4. (B–G) Time-progressive morphodynamic reconstructions of flow and bed. Note that only the basal flow is depicted and not the overriding low-density flow nor the ambient sea water. Note preservation of the downstream lee side deposits (arrow in (B)). Time span (B–G) is of the order of a few hours (Table 1).

4.3. Dune cross-bedded clinoform units

4.3.1. Sedimentary features

Backset-bedded clinoform units are enveloped by stacks of high-angle cross-bedded sets, comprising ca. 50% of the studied carbonate ramp succession (Fig. 2). Such dune cross-bedded clinoform units were formed by the action of subaqueous dunes, which migrated slightly oblique down the ramp slope (Fig. 1) as a result of southeastward currents that underwent an apparent deflection to the right due to the Coriolis force (cf. Puga-Bernabéu et al., 2010; Massari and D'Alessandro, 2012). A single high-angle cross-bed (up to 10 cm thick, dipping up to 30 degrees) is bounded by the highest-order surface in a clinoform unit and is deposited from an individual grainflow down the lee-side of a small- to medium-scale dune (*sensu* Ashley, 1990). Such dunes encompassed parasitic bedforms that migrated over the stoss-side of a large-scale (*sensu*

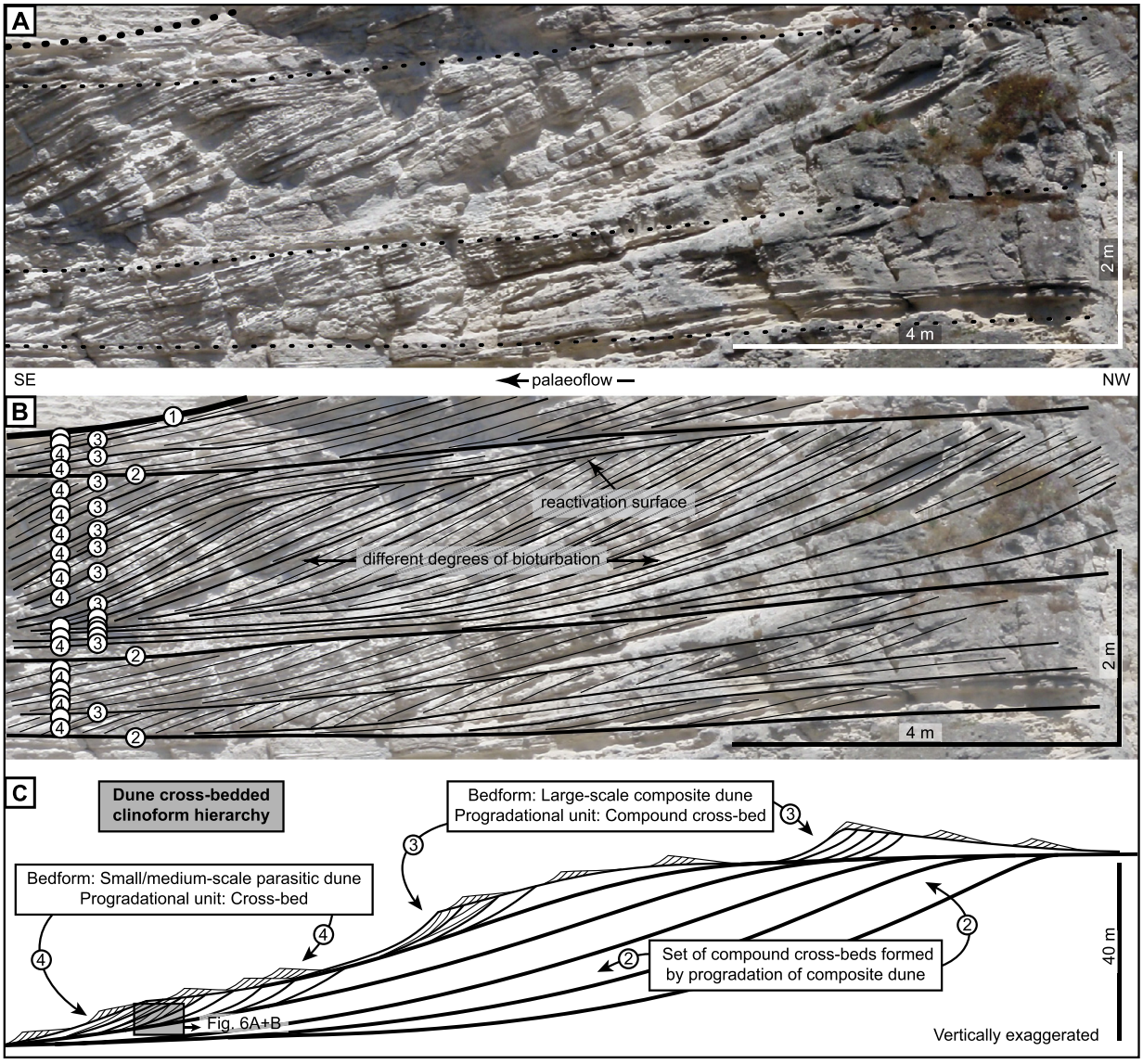

Fig. 6. Close-up of high-angle cross-stratification formed by the migration of subaqueous dunes. For location see Fig. 2. (A) Photo panel. Dotted lines indicate unit boundaries. (B) Line drawing of internal stratification. Encircled numbers have similar meaning as those in Fig. 2. (C) Conceptual model for the formation of dune cross-bedded clinoform units by the progradational stacking of large-scale composite dunes.

Ashley, 1990) parent bedform, forming compound cross-beds on the lee-side of such composite dunes (Fig. 6). Composite dunes had a high preservation potential once they migrated below storm wave base and down the ramp slope, where they would ultimately be preserved as compound cross-bedded sets. Advancement of the carbonate ramp occurred by the progradational stacking of such sets (Figs. 1C, 6C). The formation of a single dune cross-bedded clinoform unit finished with the blanketing of the ramp slope during the rapid deposition of a backset-bedded clinoform unit from a high-energy gravity flow.

Based on the variation in bed thickness, the presence of numerous reactivation surfaces and different degrees of *Thalassinoides* bioturbation (Fig. 6), dune cross-bedded clinoform units clearly reflect a polycyclic evolution. The number of distinct 'dune-activating events' within a single clinoform unit is estimated from outcrop between 50 and 500. The average recurrence period of backset-generating events also constrains the average time contained within single dune cross-bedded clinoform units at 14–35 kyr. This estimated overall duration and the number of dune-activating events, imply that on average subaqueous dunes were active only once every 46 to 458 years (Table 2).

4.3.2. Palaeohydraulic reconstruction

Previous studies have shown that dune migration on the Mediterranean shelf is locally related to strong, sustained winds capable of moving the entire water column (e.g. Bassetti et al., 2006). The height of the water column must have exceeded the preserved clinoform height by at least the depth of the storm wave base (Pomar and Tropeano, 2001), hence water depth is estimated at 50 to 100 m. Flow velocities required to form subaqueous dunes in sands with the measured grain size distribution (median grainsize $D_{50} = 1.0$–2.0 mm) were calculated, using the scale-independent bedform stability diagram of Van den Berg and Van Gelder (1993), to range from 1.4 to 2.7 m/s for such water depths (Table 1).

Subaqueous dunes form only under bed-load-dominated flows, as high sediment concentrations suppress their formation (Wan and Wang, 1994). For bed-load-dominated flows, the dimensionless sediment flux q_{s*} can be estimated using bed-load predictors, e.g. Meyer-Peter and Mueller (1948);

$$q_{s*} = 8\left(\theta' - \tau_{cr*}\right)^{3/2} \quad (4)$$

Table 2
Time comprised within the depositional system, backset-bedded clinoform units and dune cross-bedded clinoform units, and the average recurrence period of backset-generating events and dune-activating events.

	Unit	Lower limit		Mean	Upper limit	
		95% CI[1]	68% CI[2]		68% CI[2]	95% CI[1]
Depositional system						
Time comprised within studied clinoform succession (20 clinoform couplets)	kyr	287	364	458	573	705
Backset-bedded clinoform units						
Average time comprised within single clinoform couplet, i.e. average recurrence period backset-generating events	kyr	14.3	18.2	22.9	28.6	35.3
Dune cross-bedded clinoform units						
Average recurrence period, $n = 50$ dune-activating events	yr	287	364	458	573	705
Average recurrence period, $n = 500$ dune-activating events	yr	29	36	46	57	71

[1,2] CI: Confidence Interval. Lower and upper limits of 95% (68%) confidence interval correspond to 47.5% (34%) on either side of the mean at 2.5% (16%) and 97.5% (84%) cumulative probability density. See Fig. 3B for visual representation.

where the critical Shield stress required for the initiation of motion is $\tau_{cr*} = 0.047$ for well sorted, fine gravel and θ' is the non-dimensional mobility parameter (Van Rijn, 1984). The latter ranges from 0.15 to 1.5 for subaqueous dunes in the observed grain size distribution (Van den Berg and Van Gelder, 1993). However, values above $\theta' = 0.5$ yield unrealistically high flow velocities (>3.0 m/s) when compared to modern environments (e.g. Kubicki, 2008; Barrie et al., 2009) and were therefore not considered in the calculations. The non-dimensional sediment flux q_{s*} is dimensionalised by

$$q_s = q_{s*} D_{50} \sqrt{\left(\frac{\rho_{sed} - \rho_{amb}}{\rho_{amb}}\right) g D_{50}} \quad (5)$$

where ρ_{sed} and ρ_{amb} are the densities of the sediment (2700 kg/m^3) and the ambient water. Cumulative flow duration for dune cross-bedded clinoform units is estimated by dividing the dip-parallel, cross-sectional area of the clinoform unit A by sediment flux q_s. It follows that for the deposition of one dune cross-bedded clinoform unit of dimensions similar to those of the examined backset-bedded clinoform unit, the cumulative flow duration is 1.25 ± 1 yr (Table 1). This implies that individual dune-activating events, of which 50 to 500 together generated a single dune cross-bedded clinoform unit, lasted between approximately 5 hours and 2 weeks (Table 1).

5. Discussion

5.1. Palaeogeography of the Favignana carbonate ramp

The age constraints produced here enable the reconstruction of the system dynamics of the Favignana carbonate ramp, thereby resolving its place in the framework of the Pleistocene sequences of Sicily (Catalano et al., 1998). The major source of skeletal hash was almost certainly a vast carbonate factory on the inferred sill between the tectonic ridges of the islands of Favignana and Levanzo, NW of the studied clinoform succession as hinted by the SE ramp slope progradation and mean dip of subaqueous dune cross-beds. The statistically robust age model, developed from strontium isotope stratigraphy, brackets the period of major clinoform progradation between 1.6 ± 0.1 and 1.1 ± 0.1 Ma (95% confidence level). The time comprised within the Favignana system, spanning several hundred kyr, refutes a 41-kyr orbital obliquity-controlled genesis as proposed for the clinoform successions of the Lower Pleistocene of Sicily (Catalano et al., 1998; Massari and D'Alessandro, 2012). This is in line with the generally greater length, height and thickness of the Favignana clinoform units compared to those of the carbonate ramp successions of Sicily. The latter, forming well-developed carbonate sequences up to ca. 30 m thick (e.g. Massari and D'Alessandro, 2012), are particularly preserved between 2.5–2.1 Ma and between 1.6–0.8 Ma (Catalano et al., 1998).

Although the clinoform succession of present-day Favignana is incomplete and extended NW towards the carbonate factory, one can argue that, within error, the onset of major progradation of the Favignana carbonate ramp correlates to the important sequence boundary at 1.6 Ma, which formed as the result of a eustatic lowstand (Wornardt and Vail, 1991; Catalano et al., 1998). The resulting global regression created wide-spread hiatuses in the onshore basins of, in particular, western Sicily (Catalano et al., 1998), which apparently coincided with the commencement of carbonate production in the Favignana system. On the basis of available data, it is tentatively suggested that the major sea-level lowstand at ca. 1.6 Ma placed the submarine high between Favignana and Levanzo in a position favourable to the onset of heterozoan carbonate production. In the subsequent 0.3–0.7 Myr, the combination of aggradation, tectonic uplift and long-term sea-level rise apparently maintained such conditions whilst preventing subaerial exposure of the carbonate factory during high-frequency lowstands. This resulted in the continuous progradation of the Favignana carbonate ramp in the absence of any recognisable obliquity-forced signature.

5.2. Decennial to centennial storms

The formation and migration of subaqueous dunes in present-day shelf environments result from strong bottom currents (0.8–1.9 m/s, e.g. Kubicki, 2008; Barrie et al., 2009) related to tides (Barrie et al., 2009), strong winds (Kubicki, 2008; Barrie et al., 2009), sinking dense water masses (Lykousis, 2001) or ocean water circulation patterns (Flemming, 1978). Numerous studies deal with modern subaqueous dunes that are active exclusively during extreme storms (e.g. Bassetti et al., 2006; Li and King, 2007; Kubicki, 2008; Lo Iacono et al., 2010). Numerical modelling by Bassetti et al. (2006) on the outer shelf of the Gulf of Lions (western Mediterranean) shows that a single day of 20 m/s wind, with a recurrence period of 4 yr, is sufficient for the erosion and transport of fine-grained sand at 100 m water depth. According to these authors, there is "no doubt that much more severe meteorological conditions allow episodic transport of all classes of sand and rejuvenation of subaqueous dunes".

The calculated flow velocities for the formation of subaqueous dunes in the Favignana system (1.4–2.7 m/s) are comparable to the range of values measured in modern environments. The Aegadian Archipelago is at present not affected by significant tidal currents, nor by the movement of large water masses, similar to the conditions that are believed to have prevailed throughout the Early Pleistocene. The influence of strong winds in the modern Mediterranean region, on the other hand, was assessed by Trigo et al.

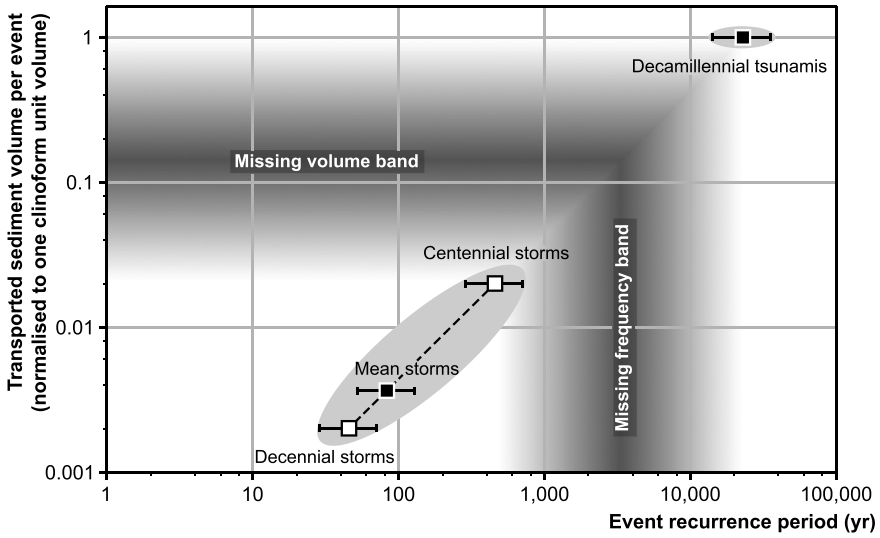

Fig. 7. Conceptual log–log-plot displaying transported sediment volume per event (normalised to one clinoform unit volume) versus event recurrence period. The lack of overlap between the two populations confirms that the events associated with the deposition of dune cross-bedded clinoform units genetically differ from the events related to the generation of backset-bedded clinoform units. See also Table 3.

(1999), who showed that over an 18 year-period less than 10% of the storms lasted more than one day and very rarely exceeded two days in duration. Winds capable of generating bottom currents sufficiently powerful to initiate the motion of coarse-grained carbonate sand must have surpassed the 20 m/s wind velocity threshold of Bassetti et al. (2006) for fine-grained sand. Only 1% of the European winter storms reach maximum near-surface wind speeds over 20 m/s and only 0.1% over 26 m/s (Leckebusch et al., 2006). Modelling results of Leckebusch et al. (2006) show that around present-day Sicily ten storms per winter occur. If the threshold for the initiation of motion is placed at 26 m/s, sediment transport on the Favignana carbonate ramp only took place during 0.1% of the storms (based on modern-day conditions), which implies subaqueous dune activity approximately once every 100 yr. According to Sabatier et al. (2012), periods of increased storminess in the northwestern Mediterranean Sea were in phase with cold events recorded in the North Atlantic over the past 7 kyr, suggesting that, during the colder Pleistocene climate, Mediterranean storm activity was more intense than today.

The infrequent events associated with the dune cross-bedded clinoform units occurred about once every 46 to 458 yr and lasted approximately between ca. 5 hours and two weeks (Tables 1, 2). Storm-related, wind-induced currents between the two palaeoislands were probably enhanced by funnelling, generating bottom current velocities of around 2 m/s (Table 1). Based on a comparison with the recent Mediterranean region, such events scale in intensity, duration and recurrence period with rare, extreme storms. The subaqueous dunes that formed half of the Favignana carbonate ramp deposits were thus typically inactive on a daily basis and were reactivated only during major decennial to centennial storms (Fig. 7, Table 3).

5.3. Millennial to decamillennial tsunamis

A clinoform couplet represents on average about 14–35 kyr. Half of it is formed by the stacking of subaqueous dunes during repeated events that cumulatively covered some hundreds of days. The remaining half consists of one thick backset-bedded clinoform unit, deposited during a single flow event that lasted no more than a few hours. This implies a two to four orders of magnitude difference in average sedimentation rate between the two types of deposits. A similar magnitude difference is observed in the associated average event-recurrence period: 46–458 yr for dune-activating events and 14–35 kyr for backset-generating events. The missing frequency band in the recurrence period of events capable of transporting skeletal sand and gravel down the ramp slope, indicates that the events related to each type of clinoform unit belong to two genetically different populations (Fig. 7). Hence, supercritical flow-generation cannot be linked to extreme storms (cf. Hansen, 1999; Pomar et al., 2002; Andreetta et al., 2008; Massari and D'Alessandro, 2012) and must be associated with rare events of greater magnitude.

One type of catastrophic event capable of rapid mobilisation of large quantities of sediment is a slope-edge collapse, which could be induced by oversteepening, seismic-related liquefaction, or pore-water overpressure resulting from a severe, storm-produced drop in atmospheric pressure and associated local sea-level rise. However, there is no evidence in the studied carbonate ramp succession, such as extensive soft-sediment deformation or large failure surfaces, to support such a hypothesis.

The possible role of tsunamis in generating backset-stratification was already stressed by Andreetta et al. (2008). The assumption that certain submarine gravity-flow beds record tsunamis (Arai et al., 2013, and refs. therein) is in agreement with the observations from Favignana Island. Although tsunamis are less frequent in the Mediterranean Sea than in the world oceans, there is an extensive database covering more than 2000 yr of historical accounts of Mediterranean tsunami events (Papadopoulos and Fokaefs, 2005). Tsunamis originate from earthquakes, volcanic eruptions, landslides and meteor impacts, of which earthquakes are expected to cause at least 75% of the tsunamis in the Mediterranean Sea (Lorito et al., 2008; Sørensen et al., 2012). The most important contributor to tsunamis in the Mediterranean region is the Hellenic Arc subduction zone in the eastern part of the basin (Lorito et al., 2008). However, travelling tsunamis are incapable of passing the Strait of Sicily (Sørensen et al., 2012). Consequently, the western Mediterranean Sea has a lower tsunami potential than the eastern part of the basin, with less active source zones along the north Algerian coast and around Sicily (Lorito et al., 2008).

Papadopoulos and Fokaefs (2005) evaluated the maximum intensity of 140 reliable tsunami events in the Mediterranean region from historical documentary sources. They found that over the past 700 yr the Mediterranean Sea experienced five very strong, "destructive" tsunamis, three of which occurred in the eastern Mediterranean region and two in the Messina Strait between Sicily and Italy. The authors admit the possible incompleteness of the

Table 3
Characteristics of storm and tsunami events of different orders of magnitude affecting the Pleistocene Favignana carbonate ramp.

Events			Signature on ramp top			Signature on ramp slope		
	Type	Recurrence time scale	Waves	Induced currents	Sediment transport (erosion)	Induced currents	Bedforms	Deposits
Dune cross-bedded clinoform units	Minor storm	Annual	Little storm waves	Limited wind-induced current	Minor agitation, hardly any sediment transport	None	No bedform generation or reworking	No deposition
	Major storm	Decennial	Big storm waves	Weak, short-lived, wind-induced current	Considerable agitation, minor sediment transport	Weak, unidirectional flow of the entire water column (subcritical, Fr < 1)	Small-scale generation and reactivation of subaqueous dunes	Small amounts of high-angle, dune cross-bedded deposits
	Extreme storm	Centennial	Extremely big storm waves	Strong, long-lasting, wind-induced current	Severe agitation, major sediment transport	Strong, unidirectional flow of the entire water column (subcritical, Fr < 1)	Large-scale generation and reactivation of subaqueous dunes	Large amounts of high-angle, dune cross-bedded deposits
Backset-bedded clinoform units	Minor tsunami	Centennial	Very low tsunami-wave	No wave shoaling-induced current	No sediment transport	None	No bedform generation or reworking	No deposition
	Major tsunami	Millennial	Low tsunami-wave	Minor wave shoaling-induced current	Major sediment transport	Minor sediment gravity flow travelling down-ramp (possibly supercritical, Fr > 1)	Possibly minor erosion and generation of upper-stage plane bedding and/or antidunes (no preservation)	Minor gravity flow bed (cm/dm-scale thickness), to be reworked into subaqueous dunes during later storm activity
	Extreme tsunami	Decamillennial	High tsunami-wave	Major wave shoaling-induced current	Extreme sediment transport	Major sediment gravity flow travelling down-ramp (supercritical, Fr > 1)	Major erosion and generation of (breaking-wave) antidunes	Major gravity flow bed (metre-scale), top to be reworked into subaqueous dunes during later storm activity[1]

[1] The amount of sediment reworked from upper part of major gravity-flow bed equals approximately the amount of material eroded by the gravity flow.

list and note that the observation period is short with respect to the rareness of events, rendering the dataset not very suitable for estimation of the recurrence period of very strong tsunamis in the western Mediterranean Sea. Moreover, it is problematic to use data derived from local historical sources to assess the probability of a fixed geographical location to encounter a tsunami event.

A different strategy was adopted by Sørensen et al. (2012), producing a synthetic catalogue of 100-kyr duration that contains all potentially tsunamigenic earthquakes in the Mediterranean region. This allows the calculation of the frequency with which a predefined tsunami amplitude threshold is exceeded for every point in the Mediterranean Sea. It follows that all Mediterranean sites are prone to tsunami events, of which the amplitude increases with decreasing probability level (i.e. with increasing recurrence period). Most notably, the modelling results reveal that the Favignana carbonate ramp experienced tsunami waves exceeding several metres with an annual probability level below 0.0001, corresponding to a recurrence period greater than 10 kyr (cf. Sørensen et al., 2012).

In case of tsunamis approaching shorelines, wave shoaling processes may lead to considerable inland penetration of major surges (Joseph, 2011). Tsunami-related deposits in onshore environments, however, have a very low preservation potential due to the typical reworking in such settings. Nevertheless, some studies document, for example, “mega-tsunami overwash” deposits intercalated within early Holocene aeolianites along the Mediterranean coast of Tunisia, containing concave-up scours filled with internal geometries mimicking swaley cross-stratification (Frébourg et al., 2010). Likewise, a low preservation potential of tsunami deposits is commonly attributed to the shallow-marine environment, albeit that field observations from in particular the Pliocene of southern Italy exist (Massari and D’Alessandro, 2000; Massari et al., 2009). These deposits originated in a restricted-bay environment, encompassing scour-and-drape structures of up to more than 50 m in wavelength, interpreted to have resulted from landward tsunami surges that subsequently swept back offshore (Massari and D’Alessandro, 2000). Such “flows of exceptional energy” were characterised by multiple pulses, reflecting the impact of trains of tsunami waves. The erosive power of the catastrophic events is testified by the presence of transported remains of infaunal benthic organisms that lived deep within the sea bed, suggesting the removal of the upper few dm of the middle-inner shelf floor (Massari et al., 2009).

The single gravity-flow beds that compose the backset-bedded clinoform units of the Favignana carbonate ramp are proposed to have resulted from rare tsunami events with an average recurrence period on a decamillennial time scale. The effect of tsunamis, however, is different from that in the above described examples; in the Favignana system there were no onshore surges and associated return flows involved in the formation of ramp slope deposits. Here, the passing of tsunami waves over the submerged ramp top, situated on a submarine high between two islands and which hosted the most important carbonate factory of the Favignana system, is of pivotal importance.

In the deep waters of the source zone (western Mediterranean Sea), tsunami waves assumed a symmetrical, sinusoidal form characterised by a high propagation velocity (hundreds of km/h), a long wavelength (hundreds of km) and a long period (up to an hour). Upon experiencing progressively shallower water depths when approaching the Sicilian shelf from the west, tsunami waves adopted a more asymmetrical and solitary form, accompanied by a rapid decrease in flow velocity and wavelength under continuously growing wave height and steepness. Wave period, however, remained unaltered (cf. Joseph, 2011). Such wave shoaling processes resulted in the generation of a flow over the carbonate factory (Fig. 1D), in the direction of wave propagation, during half of the wave period (i.e. between the passage of the wave trough and the passage of the wave crest) spanning some tens of min-

utes. Wave shoaling, in this case, is not necessarily accompanied by wave breaking and surge formation, which depend largely on wave steepness (cf. Joseph, 2011).

The sediment transport (erosion) capacity of such a flow depends on the energy budget of the tsunami wave upon reaching the Favignana ramp top. Similar to the threshold of the initiation of sediment motion by storm-driven, wind-induced currents, there is a threshold for tsunami intensity leading to shoaling-induced flows powerful enough to transport skeletal material over the ramp top. In addition, flow strength of tsunami currents may be significantly enhanced by funnelling between the two islands.

Table 3 shows a relative tsunami intensity scale, comprising minor, major and extreme tsunamis with a recurrence period of increasing order of magnitude. Only major and extreme tsunamis, recurring on time scales of kyr and tens of kyr, were capable of major and extreme sediment transport over the ramp top. During major tsunami events high amounts of skeletal hash were transported towards the outer limits of the carbonate factory, where the massive dumping of material at the edge of the ramp slope resulted in the formation of a sediment gravity flow. Such deposits, however, were of insufficient thickness to be preserved and subsequent reworking occurred during the next episode of subaqueous dune activity. Only the very rare tsunamis of extreme intensity, recurring on decamillennial time scales, possessed the power to deliver gigantic amounts of carbonate debris at the ramp slope, resulting in the generation of major, supercritical sediment gravity flows that deposited anomalously thick, backset-bedded clinoform units (Fig. 1D). Such units have a variable thickness due to the variation in the energy budget of the most extreme events. The time between two extreme tsunami events is also relevant, since, once devastated, the carbonate factory required sufficient time to recover and to build up a new stock of carbonate sand.

6. Conclusions

The calcarenites and calcirudites of Favignana Island consist of a prograding carbonate ramp succession of alternating subaqueous dune deposits and anomalously thick backset-bedded gravity-flow units. Hydraulic calculations reveal that these deposits record a very non-linear sedimentation history, which is not in line with the gradual build-up commonly assumed for carbonate ramps. The age of the Favignana ramp succession was measured for the first time in this study, showing that in terms of sediment transport the ramp was practically inactive during the vast majority of time (~99.99%), with cumulative 2 yr (~0.01%) of decennial to centennial storm-induced currents depositing half of the sediments per 14–35 kyr. An equal amount of material was resedimented during catastrophic tsunami events with a decamillennial recurrence period. Such tsunamis were detrimental to the carbonate factory, sweeping enormous amounts of material off the ramp top in no more than a few hours. We contend that the frequent occurrence of thick, predominantly backset-bedded bodies in Mediterranean carbonate successions indeed indicates a catastrophic evolution, which is a new way to interpret such fossil carbonate ramps.

Acknowledgements

The Société de Physique et d'Histoire Naturelle de Genève is thanked for providing a Bourse A. Lombard Fund to A. Slootman. The authors are indebted to Jort Koopmans and Frits Hilgen for foraminifera determination. Agathe Martignier is thanked for her guidance during SEM analysis, and Michèle Senn for her help with sample preparation for Sr isotope analysis. The manuscript greatly benefited from the fruitful discussion with Judith ter Schure on statistical treatment of Sr isotope data. The authors gratefully acknowledge editor Martin Frank, and Claude Colombié and two anonymous reviewers for their constructive comments on the initial version of the manuscript.

Appendix A. Supplementary material

Supplementary material related to this article can be found online at http://dx.doi.org/10.1016/j.epsl.2016.03.052.

References

Ahr, W.M., 1973. The carbonate ramp – an alternative to the shelf model. Trans. Gulf Coast Assoc. Geol. Soc. 23, 221–225.
Alexander, J., Fielding, C., 1997. Gravel antidunes in the tropical Burdekin River, Queensland, Australia. Sedimentology 44, 327–337.
Andreetta, R., Morsilli, M., Pomar, L., 2008. Sedimentological features of coarse-grained deep water backset beds in a distally steepened carbonate ramp (Late Miocene, Menorca, Balearic Islands, Spain). Rend. Onl. Soc. Geol. Ital. 2, 19–22.
Arai, K., Naruse, H., Miura, R., Kawamura, K., Hino, R., Ito, Y., Inazu, D., Yokokawa, M., Izumi, N., Murayama, M., Kasaya, T., 2013. Tsunami-generated turbidity current of the 2011 Tohoku-Oki earthquake. Geology 41, 1195–1198.
Ashley, G.M., 1990. Classification of large-scale subaqueous bedforms: a new look at an old problem – SEPM bedforms and bedding structures. J. Sediment. Res. 60, 160–172.
Bagnold, R.A., 1954. Experiments on a gravity-free dispersion of large solid spheres in a Newtonian fluid under shear. Proc. R. Soc. Lond. Ser. A 225, 49–63.
Barrie, J.V., Conway, K.W., Picard, K., Greene, H.G., 2009. Large-scale sedimentary bedforms and sediment dynamics on a glaciated tectonic continental shelf: examples from the Pacific margin of Canada. Cont. Shelf Res. 29, 796–806.
Bassetti, M.A., Jouet, G., Dufois, F., Berné, S., Rabineau, M., Taviani, M., 2006. Sand bodies at the shelf edge in the Gulf of Lions (Western Mediterranean): deglacial history and modern processes. Mar. Geol. 234, 93–109.
Carannante, G., Simone, L., 1988. Foramol carbonate shelves as depositional site and source area: recent and ancient examples from the Mediterranean region. AAPG Bull. 72, 993–994.
Cartigny, M.J.B., Eggenhuisen, J.T., Hansen, E.W.M., Postma, G., 2013. Concentration-dependent flow-stratification in experimental high-density turbidity currents and their relevance to turbidite facies models. J. Sediment. Res. 83, 1046–1064.
Cartigny, M.J.B., Ventra, D., Postma, G., Van den Berg, J.H., 2014. Morphodynamics and sedimentary structures of bedforms under supercritical-flow conditions: new insights from flume experiments. Sedimentology 61, 712–748.
Catalano, R., Di Stefano, E., Sulli, A., Vitale, F.P., Infuso, S., Vail, P.R., 1998. Sequences and systems tracts calibrated by high-resolution bio-chronostratigraphy: the central Mediterranean Plio-Pleistocene record. SEPM Spec. Publ. 60, 155–177.
Catalano, R., Merlini, S., Sulli, A., 2002. The structure of western Sicily, central Mediterranean. Pet. Geosci. 8, 7–18.
Flemming, B.W., 1978. Underwater sand dunes along the southeast African continental margin – observations and implications. Mar. Geol. 26, 177–198.
Frébourg, G., Hasler, C.A., Davaud, E., 2010. Catastrophic events recorded among Holocene eolianites (Sidi Salem Formation, SE Tunesia). Sediment. Geol. 224, 38–48.
Hand, B.M., 1974. Supercritical flow in density currents. J. Sediment. Res. 44, 637–648.
Hansen, K.S., 1999. Development of a prograding carbonate wedge during sea level fall: lower Pleistocene of Rhodes, Greece. Sedimentology 46, 559–576.
Hiscott, R.N., 1994. Traction-carpet stratification in turbidites – fact or fiction? J. Sediment. Res. 64, 204–208.
James, N.P., 1997. The cool-water carbonate depositional realm. SEPM Spec. Publ. 56, 1–20.
Joseph, A., 2011. Tsunamis: Detection, Monitoring, and Early-Warning Technologies. Academic Press.
Kennedy, J.F., 1963. The mechanics of dunes and antidunes in erodible-bed channels. J. Fluid Mech. 16, 521–544.
Kubicki, A., 2008. Large and very large subaqueous dunes on the continental shelf off southern Vietnam, South China Sea. Geo Mar. Lett. 28, 229–238.
Leckebusch, G.C., Koffi, B., Ulbrich, U., Pinto, J.G., Spangehl, T., Zacharias, S., 2006. Analysis of frequency and intensity of European winter storm events from a multi-model perspective, at synoptic and regional scales. Clim. Res. 31, 59–74.
Li, M.Z., King, E.L., 2007. Multibeam bathymetric investigations of the morphology of sand ridges and associated bedforms and their relation to storm processes, Sable Island Bank, Scotian Shelf. Mar. Geol. 243, 200–228.
Lo Iacono, C., Guillén, J., Puig, P., Ribó, M., Ballesteros, M., Palanques, A., Lí Farrán, M., Acosta, J., 2010. Large-scale bedforms along a tideless outer shelf setting in the western Mediterranean. Cont. Shelf Res. 30, 1802–1813.
Lorito, S., Tiberti, M.M., Basili, R., Piatanesi, A., Valensise, G., 2008. Earthquake-generated tsunamis in the Mediterranean Sea: scenarios of potential threats to Southern Italy. J. Geophys. Res. 113, B01301.
Lykousis, V., 2001. Subaqueous bedforms on the Cyclades Plateau (NE Mediterranean) – evidence of Cretan Deep Water formation? Cont. Shelf Res. 21, 495–507.

Massari, F., 1996. Upper-flow-regime stratification types on steep-face, coarse-grained, Gilbert-type progradational wedges (Pleistocene, Southern Italy). J. Sediment. Res. 66, 364–375.
Massari, F., D'Alessandro, A., 2000. Tsunami-related scour-and-drape undulations in Middle Pliocene restricted-bay carbonate deposits (Salento, south Italy). Sediment. Geol. 135, 265–281.
Massari, F., D'Alessandro, A., 2012. Facies partitioning and sequence stratigraphy of a mixed siliciclastic-carbonate ramp stack in the Gelasian of Sicily (S Italy): a potential model for icehouse, distally-steepened heterozoan ramps. Riv. Ital. Paleontol. 118, 503–534.
Massari, F., D'Alessandro, A., Davaud, E., 2009. A coquinoid tsunamite from the Pliocene of Salento (SE Italy). Sediment. Geol. 221, 7–18.
McArthur, J.M., Howarth, R.J., Shields, G.A., 2012. Strontium isotope stratigraphy. In: Gradstein, F.M., Ogg, J.G., Schmitz, M., Ogg, G. (Eds.), The Geologic Time Scale 2012. Elsevier, pp. 127–144.
Meyer-Peter, E., Mueller, R., 1948. Formulas for bed-load transport. Proc. Int. M. Hydr. Res. 26.
Papadopoulos, G.A., Fokaefs, A., 2005. Strong tsunamis in the Mediterranean Sea: a re-evaluation. ISET J. Earthq. Technol. 42, 159–170.
Pedley, M., Carannante, G., 2006. Cool-water carbonate ramps: a review. Geol. Soc. (Lond.) Spec. Publ. 255, 1–9.
Pomar, L., Tropeano, M., 2001. The Calcarenite di Gravina Formation in Matera (Southern Italy): new insights for coarse-grained, large-scale, cross-bedded bodies encased in offshore deposits. AAPG Bull. 85, 661–689.
Pomar, L., Obrador, A., Westphal, H., 2002. Sub-wavebase cross-bedded grainstones on a distally steepened ramp, upper Miocene, Menorca, Spain. Sedimentology 49, 139–169.
Prager, E.J., Southard, J.B., Vivoni-Gallart, E.R., 1996. Experiments on the entrainment threshold of well-sorted and poorly sorted carbonate sands. Sedimentology 43, 33–40.
Puga-Bernabéu, Á., Martín, J.M., Braga, J.C., Sánchez-Almazo, I.M., 2010. Downslope-migrating sandwaves and platform-margin clinoforms in a current-dominated, distally steepened temperate-carbonate ramp (Guadix Basin, Southern Spain). Sedimentology 57, 293–311.
Sabatier, P., Dezileau, L., Colin, C., Briqueu, L., Bouchette, F., Martinez, P., Siani, G., Raynal, O., Von Grafenstein, U., 2012. 7000 years of paleostorm activity in the NW Mediterranean Sea in response to Holocene climate events. Quat. Res. 77, 1–11.
Ślączka, A., Nigro, F., Renda, P., Favara, R., 2011. Lower Pleistocene deposits in East part of the Favignana Island, Sicily, Italy. Ital. J. Quat. Sci. 24, 153–169.
Smalley, P.C., Higgins, A.C., Howarth, R.J., Nicholson, H., Jones, C.E., Swinburne, N.H.M., Bessa, J., 1994. Seawater Sr isotope variations through time: a procedure for constructing a reference curve to date and correlate marine sedimentary rocks. Geology 22, 431–434.
Smith, D.A., Cheung, K.F., 2004. Initiation of motion of calcareous sand. J. Hydraul. Eng. 130, 467–472.
Sørensen, M.B., Spada, M., Babeyko, A., Wiemer, S., Grünthal, G., 2012. Probabilistic tsunami hazard in the Mediterranean Sea. J. Geophys. Res. 117, B01305.
Tavarnelli, E., Renda, P., Pasqui, V., Tramutoli, M., 2003. The effects of post-orogenic extension on different scales: an example from the Apennine–Maghrebide fold-and-thrust belt, SW Sicily. Terra Nova 15, 1–7.
Trigo, I.F., Davies, T.D., Bigg, G.R., 1999. Objective climatology of cyclones in the Mediterranean region. J. Climate 12, 1685–1696.
Van den Berg, J.H., Van Gelder, A., 1993. A new bedform stability diagram, with emphasis on the transition of ripples to plane bed in flows over fine sand and silt. Spec. Publ. Int. Assoc. Sedimentol. 17, 11–21.
Van Rijn, L.C., 1984. Sediment transport, part 1: bed load transport. J. Hydraul. Eng. 110, 1431–1456.
Wan, Z., Wang, Z., 1994. Hyperconcentrated Flow. Balkema, Rotterdam.
Wornardt, W.W., Vail, P.R., 1991. Revision of the Plio-Pleistocene cycles and their application to sequence stratigraphy and shelf and slope sediments in the Gulf of Mexico. Trans. Gulf Coast Assoc. Geol. Soc. 41, 719–744.